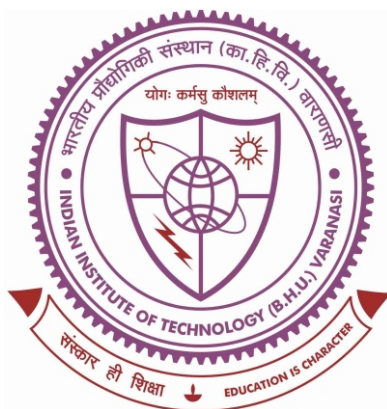


Understanding of Redox Interactions of Transition Metal Ions in Different Lattices to Develop Superior Water Splitting Electrocatalysts



Thesis submitted in partial fulfillment for the
Award of Degree

Doctor of Philosophy

By

Shraddha Jaiswal

DEPARTMENT OF CHEMISTRY
INDIAN INSTITUTE OF TECHNOLOGY
(BANARAS HINDU UNIVERSITY)
VARANASI - 221005
INDIA

Roll No. 18051504

Year 2024

***DEDICATED TO MY LOVING
PARENTS***



भारतीय
प्रौद्योगिकी
संस्थान
काशी हिन्दू विश्वविद्यालय



INDIAN
INSTITUTE OF
TECHNOLOGY
BANARAS HINDU UNIVERSITY

DECLARATION BY THE CANDIDATE

I, **Shraddha Jaiswal**, certify that the work embodied in this thesis is my own bonafied work carried out by me under the supervision of “**Dr. Asha Gupta**” from **Jan 2019** to **Dec 2024**, at the **Department of Chemistry, Indian Institute of Technology (BHU), Varanasi**. The matter embodied in this thesis has not been submitted for the award of any other degree/diploma.

I declare that I have faithfully acknowledged and given credits to the researchers wherever their works have been cited in my work in this thesis. I further declare that I have not wilfully copied any other’s work, paragraphs, text, data, results etc., reported in journals, books, magazines, reports, dissertations, theses etc., or available at websites and have not included them in this thesis and have not cited as my own work.

Date: 24/12/24
Place: IIT (BHU), Varanasi

Shraddha Jaiswal
(Ms. Shraddha Jaiswal)

CERTIFICATE BY THE SUPERVISOR

It is certified that the above statement made by the student is correct to the best of my/our knowledge.

Dr. Asha Gupta
(Supervisor)
Assistant Professor,
Department of Chemistry
Indian Institute of Technology (BHU)
Varanasi-221005, (U.P.), India

Dr. Preetam Singh
(Co-Supervisor)
Associate Professor,
Department of Ceramic Engineering
Indian Institute of Technology (BHU)
Varanasi-221005, (U.P.), India

Head of the Department
Department of Chemistry
Indian Institute of Technology (BHU)
Varanasi-221005, (U.P.), India
Varanasi-221005 / Varanasi-221005



भारतीय
प्रौद्योगिकी
संस्थान
काशी हिन्दू विश्वविद्यालय



INDIAN
INSTITUTE OF
TECHNOLOGY
BANARAS HINDU UNIVERSITY

CERTIFICATE

It is certified that the work contained in the thesis entitled "*Understanding of Redox Interactions of Transition Metal Ions in Different Lattices to Develop Superior Water Splitting Electrocatalysts*" by "SHRADDHA JAISWAL" has been carried out under my supervision and that this work has not been submitted elsewhere for a degree.

It is further certified that the student fulfilled all the requirements of the comprehensive examination, candidacy and SOTA for the award of Ph.D. degree.

Dr. Asha Gupta
(Supervisor)

Assistant Professor,
Department of Chemistry
Indian Institute of Technology (BHU)
Varanasi-221005, (U.P.), India

Dr. Preetam Singh
(Co-Supervisor)

Associate Professor,
Department of Ceramic Engineering
Indian Institute of Technology (BHU)
Varanasi-221005, (U.P.), India

Head of the Department
Department of Chemistry
Indian Institute of Technology
(BHU) Varanasi-221005, (U.P.),
India



भारतीय
प्रौद्योगिकी
संस्थान
काशी हिन्दू विश्वविद्यालय



INDIAN
INSTITUTE OF
TECHNOLOGY
BANARAS HINDU UNIVERSITY

COPYRIGHT TRANSFER CERTIFICATE

Title of the thesis: *“Understanding of Redox Interactions of Transition Metal Ions in Different Lattices to Develop Superior Water Splitting Electrocatalysts”*

Name of the Student: SHRADDHA JAISWAL

Copyright Transfer

The undersigned hereby assigns to the Indian Institute of Technology (Banaras Hindu University), Varanasi all rights under copyright that may exist in and for the above thesis submitted for the award of the **“DOCTOR OF PHILOSOPHY”** degree.

Date: 24/12/24

Place: IIT (BHU), Varanasi

Shraddha Jaiswal
Signature of the Student
(Shraddha Jaiswal)

Note: However, the author may reproduce or authorize others to reproduce material extracted verbatim from the thesis or derivative of the thesis for the author’s personal use provided that the source and the Institute’s copyright notice are indicated.

Acknowledgement

This thesis signifies not only my work at IIT (BHU) but also the incredible journey that I have experienced throughout my tenure. The successful completion of this thesis would not have been possible without the guidance, support and contributions of several individuals. I am deeply grateful to everyone who played a role in making this thesis work a reality.

First and foremost, I would like to express heartfelt gratitude to my supervisor **Dr. Asha Gupta**, Department of Chemistry, IIT (BHU), Varanasi, for her invaluable support, continued guidance and encouragement throughout my research journey. I am thankful to her for introducing me to the unique area of specialization “Electrochemical Water Splitting”. Her constant encouragement and judicious suggestions have provided me the zeal to carry out my research work. I have been fortunate enough to be part of her group. Her suggestions and advice will always be beneficial in life, whether it is academic or nonacademic. I am very thankful to you ma'am for being a mentor academically as well as philosophically and wish to continue seek this mentorship in future life too.

I would like to express my warmest gratitude to my Co-supervisor **Dr. Preetam Singh**, Department of Ceramic Engineering, IIT (BHU) for his invaluable guidance, support and encouragement as well as his efforts for coordinating the resources that my experiments needed. I have been fortunate enough to work with him.

My sincere thank goes to my RPEC member **Prof. K. D. Mandal**, Department of Chemistry, IIT (BHU), **Dr. Kundan Kumar**, Department of Ceramic Engineering, IIT (BHU), and former RPEC member **Prof. Rajiv Prakash**, School of Material Science, IIT (BHU).

I would like to express my gratitude to the Head, Department of Chemistry, IIT (BHU), Varanasi, Prof. Sundaram Singh, former HODs Prof Y. C. Sharma and Prof. D. Tiwari for their kind support and for providing departmental facilities to carry out my research work smoothly.

I would like to acknowledge all the faculty members and the non-teaching staffs of my department for their valuable supports. I also like to acknowledge Central Instrumentation Facility (CIF), IIT(BHU) for characterization facilities.

I am grateful to my seniors Dr. Vishal Kushwaha, Dr. Vaishali Soni, Dr. Akanksha Yadav, Dr. Neeraj Mishra, Dr. Neeraj Singh, Dr. Rakesh Mondal, Dr. Abhay Narayan Singh for their suggestions and healthy discussions of my research issues. I am also thankful to my juniors Krishna, Abhijeet, Soham and Subash for making lab environment healthy.

I would also like to extend my gratitude to my all teachers/faculties and friends from my school, Bachelor's and Master's. Although they were far apart during this tenure, their direct or indirect support and motivation has guided me to reach this far.

Friends have always been my moral support and strength throughout my life. Words are way less to express my gratefulness to them but yet I would like to mention some close ones. My deepest thank goes to my friends Dr. R. Venkatesh, Dr. Priya Dey, Dr. Shreya Rastogi and Alok Dubey for supporting through thick and thin.

I am thankful and indebted to MHRD for providing me financial support during my research work.

Lastly, I would like to finish with my pillars of strength, where the most basic source of my life energy resides: "My Family". Their unconditional love and endless support throughout the years have brought me to such upright position where I am right now. I feel so lucky being my parents' daughter and am deeply grateful for everything they have done for me. I am especially thankful to my brothers (Dr. Shubham Jaiswal and Satyam Jaiswal) for always being there for me and cheering me on whenever I needed it. I am truly blessed to have them by my side.

Lastly, I want to thank almighty for each and everything.

Table of Content

	Page No.
Acknowledgement	i-ii
Table of Content	iii-vi
List of Figures	vii-xii
List of Tables	xiii
List of Abbreviation	xiv
Preface	xv-xix
Chapter 1. Introduction and Literature Review	
1.1 Energy Demand and Need for Alternative Sources of Energy	1
1.1.1 Hydrogen as a fuel.....	2
1.1.2 Electrocatalytic Water Splitting and Need for Non-Noble Metals-Based Catalysts.....	4
1.1.2.1 Hydrogen Evolution Reaction (HER).....	6
1.1.2.2 Oxygen Evolution Reaction (OER).....	8
1.1.3 Noble- Metal Based Catalysts for OER and HER.....	10
1.1.4 Non-Noble- Metal Based Catalysts for OER and HER	12
1.2 Transition Metal Oxides.....	13
1.2.1 Regulation Strategies.....	14
1.2.1.1 Defect Engineering.....	14
1.2.1.2 Anion Defect.....	15
1.2.1.3 Cation Defects.....	15
1.2.1.4 Doping Effects.....	15
1.2.2 ABO ₃ - type Perovskites and Ilmenite Structures.....	16
1.2.3 Perovskites Oxides.....	18
1.2.3.1 Simple Perovskites	18
1.2.3.2 Double Perovskites	19
1.2.3.3 Ruddlesden–Popper-type oxides.....	20
1.3 Key Performance Evaluating Parameters for HER and OER.....	21
1.3.1 Overpotential (η).....	21

1.3.2	Tafel Slope.....	23
1.3.3	Electrochemically Active Surface Area (ECSA)	24
1.3.4	Turnover Frequency (TOF)	25
1.3.5	Faradaic Efficiency (FE)	26
1.3.6	Mass Activity and Specific Activities.....	27
1.3.7	Screening an Electrocatalyst for Stability.....	28
1.4	Motivation and Objective of this Work.....	30
1.5	References.....	31

Chapter 2. Synthesis and Characterization Techniques

2.1	Introduction.....	41
2.2	Material Synthesis Techniques.....	41
2.3	Synthetic Methods of Transition Metal Oxides.....	41
2.3.1	Solution-Based Methods.....	42
2.3.1.1	Sol-gel Synthesis Method.....	42
2.3.1.2	Co-Precipitation.....	43
2.3.1.3	Hydrothermal/Solvothermal Synthesis.....	43
2.4	Material Characterization Techniques.....	44
2.4.1	Powder X-ray Diffraction (XRD).....	44
2.4.2	Fourier Transform Infrared (FTIR) Spectroscopy.....	44
2.4.3	Raman Spectroscopy.....	44
2.4.4	UV-Visible Spectrophotometer.....	45
2.4.5	Scanning Electron Microscopy (SEM).....	45
2.4.6	Energy Dispersive X-ray Spectroscopy (EDS or EDX).....	45
2.4.7	Transmission Electron Microscopy (TEM).....	46
2.4.8	X-ray Photoelectron Spectroscopy.....	46
2.4.9	Inductively Coupled Plasma Mass Spectrometry (ICP-MS)	46
2.4.10	BET (Brunner-Emmett-Teller) Surface Area Measurement.....	47
2.5	Electrochemical Characterization.....	47
2.5.1	Catalyst Ink Preparation and Electrode Fabrication.....	47
2.5.2	Electrochemical Setup.....	48
2.5.3	Electrochemical Characterization Techniques.....	48
2.5.3.1	Cyclic Voltammetry (CV).....	49

2.5.3.2	Linear Sweep Voltammetry (LSV).....	49
2.5.3.3	Electrochemical Impedance Spectroscopy (EIS).....	50
2.5.3.4	Chronoamperometry.....	50
2.6	References.....	51

Chapter 3. Role of Cation Deficiency and the Inductive Effect in Ti-Doped NiO for Developing Superior Electrocatalysts for the Oxygen Evolution Reaction

3.1	Introduction.....	53
3.2	Experimental Section.....	56
3.2.1	Material Synthesis.....	56
3.3	Results and Discussion.....	56
3.3.1	XRD Studies and Rietveld Refinement.....	56
3.3.2	Raman Analysis.....	59
3.3.3	FT-IR Analysis.....	60
3.3.4	XPS and ICP Analysis.....	61
3.3.5	Microstructural Analysis (SEM and TEM).....	64
3.3.6	Electrochemical Studies.....	68
3.3.6.1	OER Performances of Synthesized Catalysts.....	68
3.3.6.2	Comparative OER Study.....	74
3.3.6.3	Mott-Schottky Analysis.....	77
3.3.6.4	Long-term Stability Test.....	78
3.3.6.5	Post OER Characterization.....	79
3.5	Conclusion.....	80
3.6	References	82

Chapter 4. Sol-gel synthesized Co-doped Ilmenite-NiTiO₃ for Oxygen Evolution Reaction: Interplay of Inductive Effect and Crystal Structure

4.1	Introduction	89
4.2	Experimental Section.....	91
4.2.1	Material Synthesis.....	91
4.3	Results and Discussion.....	92
4.3.1	XRD Studies and Rietveld Refinement.....	92
4.3.2	FTIR Analysis.....	95
4.3.3	XPS Studies.....	96

4.3.4	Microstructural Analysis (SEM and TEM)	98
4.3.5	Electrochemical Studies.....	100
4.3.5.1	OER Performances of Synthesized Catalysts.....	100
4.3.5.2	Long-term Stability Test.....	105
4.3.5.3	Post OER Characterization.....	106
4.4	Conclusion.....	107
4.5	Reference.....	109

Chapter 5. Tuning of Redox Energy of Transition-Metal Ions through the Utilization of Interlayer Potentials in Layered Perovskites: Development of a Titanium-Based Superior HER Catalyst in an Acidic Medium

5.1	Introduction.....	113
5.2	Experimental Section.....	116
5.2.1	Material synthesis.....	116
5.3	Results and Discussion.....	117
5.3.1	XRD Studies and Rietveld Refinement.....	117
5.3.2	Raman and FTIR Analysis.....	120
5.3.3	XPS Studies.....	121
5.3.4	Microstructural (SEM and TEM) and ICP Analysis	123
5.3.5	Specific Surface Area Measurement.....	125
5.3.6	UV-Vis Analysis.....	126
5.3.7	Mott–Schottky Analysis.....	126
5.3.8	Electrochemical Studies.....	130
5.3.8.1	HER performances of synthesized catalysts.....	130
5.3.8.2	Long-term Stability Test.....	135
5.4	Conclusion.....	136
5.5	References.....	138

Chapter 6 Thesis Overview and Future Perspective

6.1	Thesis Overview.....	144
6.2	Future scope.....	147

Publications and Conferences.....	149
------------------------------------------	------------

List of Tables

Table No	Description	Page No.
Table 3.1	Rietveld refined structural parameters of NTO-0, NTO-3, NTO-5, NTO-7.5 and NTO 10.	58
Table 3.2	Relative concentration of Ni and Ti in $\text{Ni}_{1-2x}\text{Ti}_x\text{O}$ ($x = 0, 0.03, 0.05, 0.075, 0.10$) from ICP analysis.	65
Table 3.3	The C_{dl} and corresponding ECSA values of all the catalysts	73
Table 4.1	The obtained lattice parameters and tolerance factor of NiTiO_3 and Co-doped NiTiO_3 samples.	95
Table 4.2	The C_{dl} and corresponding ECSA values of all the catalysts.	105
Table 5.1	Structural parameters of NaYTiO_4 based on Rietveld refinement.	119
Table 5.2	ICP- MS Result of NaYTiO_4 .	124

List of Figures

Figure No.	Figure description	Page No.
Figure 1.1	The world total primary energy consumption by fuels in 2022.	1
Figure 1.2	Global distribution of GHG emissions by different sectors.	2
Figure 1.3	Hydrogen production through different sources.	3
Figure 1.4	A sustainable pathway for the circulation of a hydrogen economy by combining renewable energy and electrochemical water splitting.	4
Figure 1.5	A typical water electrolysis cell under alkaline conditions.	5
Figure 1.6	Schematic illustration of HER pathways in acidic and alkaline solutions.	7
Figure 1.7	OER mechanism (a) in alkaline and (b) in acidic media.	9
Figure 1.8	Qualitative schematic of the Sabatier principle.	10
Figure 1.9	Theoretical overpotential for oxygen evolution vs. the difference between the standard free energy of two subsequent intermediates ($\Delta G_{O^*}^0 - \Delta G_{HO}^0$) for various binary oxides and perovskite oxide.	11
Figure 1.10	Schematic illustration of transition metal-based electrocatalysts for OER and the potential strategies for performance enhancement.	13
Figure 1.11	Regulation strategies of metal oxide-based electrocatalyst.	14
Figure 1.12	Lattice diagram of ilmenite $NiTiO_3$.	17
Figure 1.13	Sketch of a basic ABO_3 perovskite oxide structure.	19
Figure 1.14	HER activity trends of overpotential at 10 mAcm^{-2} oxide as a function of A-site ionic electronegativity.	20
Figure 1.15	Inductive effects and electron exchange interactions between A sites and B sites in perovskites from molecular orbital theory.	20
Figure 1.16	Sketch of $NaYTiO_4$ Ruddlesden–Popper-type oxide structure plotted from VESTA software.	21

Figure 1.17	A model catalyst surface that visualizes the definition of geometric activity, specific activity and mass activity	28
Figure 2.1	Schematic block diagram of sol-gel synthesis procedure.	43
Figure 3.1	(a) XRD pattern of all sol-gel synthesized NTO samples and (b) Magnified image of (200) peak.	57
Figure 3.2	Rietveld refined powder XRD patterns of all NTO samples.	58
Figure 3.3	(a) Room temperature Raman spectra of all the NTO samples, (b) intensity ratio of first-order and second-order optical phonon vibrations (I_{1LO}/I_{2LO}) varying with NTO samples and (c) FTIR spectra of NTO-0 and NTO-5 samples.	60
Figure 3.4	XPS full survey scan of (a) NTO-0 and (b) NTO-5 sample.	62
Figure 3.5	Core level XPS spectrum of (a), (b) Ni (2p), (c) Ti (2p), (d), (e) O (1s).	63
Figure 3.6	SEM micrograph of (a), (c) NTO-0 (the scale bars are 1 μm and 500 nm respectively), (b), (d) NTO-5 (the scale bars are 1 μm and 500 nm respectively), (e), (f) represents elemental mapping of individual elements (Ni, Ti, and O) present in the NTO-0 and NTO-5 sample and (g), (h) EDX spectrum of NTO-0, NTO-5.	66
Figure 3.7	Bright-field TEM image (a) NTO-0, (d) NTO-5, (b), (e) HR-TEM image lattice arrangements at the localized region for NTO-0 and NTO-5; inset shows the respective SAED patterns and (c, f) HR-TEM image with interplanar d-spacing of (200) and (111) plane for NTO-0 and NTO-5 respectively.	67
Figure 3.8	OER performance of NTO series samples $\text{Ni}_{1-2x}\text{Ti}_x\text{O}$ ($x = 0.03, 0.05, 0.075, 0.1$). (a) Linear sweep voltammograms taken at a scan rate of 5 mV s^{-1} in 1 M KOH, (b) Overpotentials at a current density of 10 mA cm^{-2} , (c) Tafel plots & (d) EIS recorded at 1.54 V vs. RHE.	69
Figure 3.9	OER performance of the NTO-5 catalyst in different concentration of KOH electrolyte with pH ranging from 13 to 14.3.	70
Figure 3.10	CV measurements in a non-faradic current region (0.86 – 0.96 V vs. RHE) at scan rates of 40, 60, 80, 100, 120 and 140 mV s^{-1} of (a) NTO-0, (b) NTO-3, (c) NTO-5, (d) NTO-7.5 & (e) NTO-10 in 1 M KOH.	71

Figure 3.11	OER performance of NTO series samples $\text{Ni}_{1-2x}\text{Ti}_x\text{O}$ ($x = 0.03, 0.05, 0.075, 0.1$). (a) Plots of capacitive current density differences $\Delta J/2$ vs. the scan rate for all NTO samples & (b) Plot of ECSA vs catalyst $\text{Ni}_{1-2x}\text{Ti}_x\text{O}$ ($x = 0.03, 0.05, 0.075, 0.1$).	72
Figure 3.12	Cyclic voltammograms of $\text{Ni}_{1-2x}\text{Ti}_x\text{O}$ catalysts with various Ti contents ($0 \leq x \leq 0.1$) were recorded at a scan rate of 5 mV s^{-1} in 1 M KOH, showing the effect of Ti doping on the pre-OER redox peaks.	73
Figure 3.13	Pictorial representation of the movement of electron density because of inductive effect, $\chi \text{Ni}^{2+/3+} = 1.367, 1.695$ respectively and $\chi \text{Ti}^{4+} = 1.730$.	74
Figure 3.14	Comparison of OER performance of NTO-5 with commercial RuO_2 as reference catalyst, linear sweep voltammograms recorded at 5 mV s^{-1} in 1 M KOH; inset showing the Tafel plot.	75
Figure 3.15	N_2 adsorption/desorption isotherm curve of NTO-5.	75
Figure 3.16	CV measurements in a non-faradic current region (0.9 -1.0 V vs. RHE) at scan rates of 50, 100, 120, 140 and 160 mV s^{-1} of (a) RuO_2 in 1 M KOH & (b) plot of capacitive current density difference average ($\Delta j/2$) vs the scan rate for RuO_2 .	76
Figure 3.17	(a) OER activity normalized by BET surface area (SA) and (b) electric double-layer capacitance (EA) of NTO-5 and RuO_2 , respectively, at an overpotential of 350 mV.	77
Figure 3.18	(a) Mott-Schottky plot for NTO-0 and NTO-5 recorded at a frequency of 100 Hz and (b) Chronoamperogram of NTO-5	78
Figure 3.19	Post-OER XRD pattern of NTO-5 electrode.	79
Figure 3.20	(a) SEM images, (b) energy-dispersive spectrum & (i-iii) element mapping of post-OER NTO-5 electrode.	80
Figure 4.1	(a) XRD pattern of all sol-gel synthesized NCTO samples (b), (c) Rietveld refined XRD profile of $\text{Ni}_{1-x}\text{Co}_x\text{TiO}_3$ ($x = 0.05, 0.1, 0.15, 0.175, 0.2, 0.25$).	94
Figure 4.2	FTIR spectra of NCTO-(0, 5, 10, 17.5, 25) samples.	96
Figure 4.3	Core level XPS spectrum of (a), (b) Ni (2p), (c), (d) Co (2p), (e) Ti (2p) (f), (g) O (1s).	97

Figure 4.4	SEM micrograph of (a) NCTO-0 (the scale bars are 1 μm), bottom two left panels represent elemental mapping of individual elements (Ni, Ti, and O) present in the NCTO-0 and (b) NCTO-17.5 (the scale bars are 1 μm), bottom two right panels represent elemental mapping of individual elements (Ni, Co, Ti, and O) present in the NCTO-17.5 sample.	98
Figure 4.5	Bright-field TEM images (a) , (b) NCTO-17.5 and (c) HR-TEM image with interplanar d-spacing of (110) plane for NTO-17.5; inset shows the SAED pattern.	99
Figure 4.6	OER performance of NCTO series samples $\text{Ni}_{1-x}\text{Co}_x\text{TiO}_3$ ($x = 0.05, 0.1, 0.15, 0.175, 0.2, 0.25$). (a) Linear sweep voltammograms taken at a scan rate of 5 mV s^{-1} in 1 M KOH, (b) Overpotentials at a current density of 10 mA cm^{-2} , (c) Tafel plots, (d) EIS recorded at 1.6 V vs. RHE.	101
Figure 4.7	Determination of double layer capacitance (C_{dl}) of NCTOs (a-g) CV measurements in a non-faradic current region (0.9-1.0 V vs. RHE) at scan rates of 20, 40, 60, 80 and 100 mV s^{-1} in 1 M KOH electrolyte.	104
Figure 4.8	(a) Plots of capacitive current density differences $\Delta J/2$ vs. the scan rate for all NCTO samples & (b) Plot of ECSA vs catalyst $\text{Ni}_{1-x}\text{Co}_x\text{TiO}_3$ ($x = 0.05 - 0.25$).	105
Figure 4.9	Chronoamperogram of NCTO 17.5 at an applied potential of 1.62 V vs. RHE for 24 hrs; inset shows the linear sweep voltammograms for the 1st, 100th, 500th, and 1000th cycle at a scan rate of 100 mV s^{-1} .	106
Figure 4.10	Post-OER XRD pattern of NCTO-17.5 electrode.	107
Figure 5.1	(i) Depicting the interlayer potential on TiO_6 octahedra or TiO_2 layer & (ii) Distortion in TiO_6 octahedra due to interlayer potential.	115
Figure 5.2	Powder XRD pattern of NaYTiO_4 with optimization of different sintering conditions.	118
Figure 5.3	(a) XRD profile of all the samples $\text{Na}_{1-x}\text{K}_x\text{YTiO}_4$ ($x = 0, 0.1, 0.2$) and $\text{NaY}_{1-y}\text{Gd}_y\text{TiO}_4$ ($y = 0.1, 0.2$), (b) Magnified image of the (311) peak & (c) Rietveld refined powder XRD pattern of NaYTiO_4	119

Figure 5.4	XRD of TiO ₂ (anatase).	120
Figure 5.5	(a) FTIR spectrum of NaYTiO ₄ & (b) Raman spectrum of NaYTiO ₄ .	121
Figure 5.6	XPS full survey scan of NaYTiO ₄ powder sample.	121
Figure 5.7	(a) Na (1s) core level spectrum, (b) Y (3d) core level spectrum, (c) comparative Ti (2p) core level spectrum of (i) as-prepared sample of TiO ₂ , (ii) as-prepared sample of NaYTiO ₄ and (iii) NaYTiO ₄ after testing (post HER) & (d) O (1s) core level spectrum peak at corresponding to lattice oxygen and adsorbed oxygen.	122
Figure 5.8	(a) HR-SEM image showing morphology of NaYTiO ₄ powder sample, (b) EDX spectrum of NaYTiO ₄ , (i-iv) corresponding elemental colour mapping of individual elements (Na, Ti, O and Y, respectively).	124
Figure 5.9	HR-SEM images of NaYTiO ₄ (i) (as-prepared) before and (ii) after HER-CA testing showing the morphology is retained after the electrochemical testing.	125
Figure 5.10	(a) HR-TEM image comprising the plane with lattice fringes; inset: SAED pattern, (b) FFT and inverse FFT of the selected region of (211) plane & (c) line profile of (211) plane with its d-spacing value.	125
Figure 5.11	(a) N ₂ adsorption/desorption isotherm curve of NaYTiO ₄ ; inset shows the pore size diameter, (b) comparative UV-vis absorption spectrum and bandgap (inset) of NaYTiO ₄ and TiO ₂ powder sample, (c) UV-vis absorption spectra of Na _{1-x} K _x YTiO ₄ (x = 0.1, 0.2) and NaY _{1-y} Gd _y TiO ₄ (y = 0.1, 0.2) catalysts & (d) corresponding Tauc plot of samples Na _{1-x} K _x YTiO ₄ (x = 0.1, 0.2) and NaY _{1-y} Gd _y TiO ₄ (y = 0.1, 0.2).	127
Figure 5.12	(a) the Mott-Schottky plot for NaYTiO ₄ and TiO ₂ & (b) Mott-Schottky plot for Na _{0.8} K _{0.2} YTiO ₄ and NaY _{0.8} Gd _{0.2} TiO ₄ recorded at a frequency of 100 Hz.	128
Figure 5.13	Schematic representation of the Ti(3d)/O(2p) orbital band for (a) NaYTiO ₄ structure and anatase TiO ₂ & (b) is for Na _{0.8} K _{0.2} YTiO ₄ and NaY _{0.8} Gd _{0.2} TiO ₄ .	129

- Figure 5.14** (a) HER LSV polarization profiles at a scan rate of 5 mV s^{-1} , (b) LSV polarization profiles of Pt/C, NaYTiO₄, NaY_{0.8}Gd_{0.2}TiO₄ and TiO₂ (c) overpotential at a current density of 10 mA cm^{-2} , (d) electrochemical impedance spectra recorded at respective overpotentials. 130
- Figure 5.15** (a) Tafel plots of Na_{1-x}K_xYTiO₄ (x= 0, 0.1, 0.2) and NaY_{1-y}Gd_yTiO₄ (y = 0.1, 0.2) (b) comparative Tafel plots for Pt/C, NaYTiO₄, NaY_{0.8}Gd_{0.2}TiO₄ & TiO₂, (c) steady-state polarisation curve of NaYTiO₄ recorded by holding the given potential for 60 sec & (d) Tafel slope of NaYTiO₄ calculated from chronoamperometry. 133
- Figure 5.16** (a) CV measurements in a non-faradaic current region (0.709-0.809 V vs. RHE) at different scan rates, (b) plot of scan rate vs. capacitive current density differences (ΔJ) for NaYTiO₄ and (b) chronoamperogram of NaYTiO₄ at an applied potential of -0.15 V vs. RHE. 136

List of Abbreviations

XRD- X-ray Diffraction

HR-SEM- High-Resolution Scanning Electron Microscope

HR-TEM- High-Resolution Transmission Electron Microscope

EDX or EDS- Energy Dispersive X-ray Spectroscopy

SAED- Selected Area Electron Diffraction

FTIR- Fourier Transform Infrared Spectroscopy

XPS- X-ray Photoelectron Spectroscopy

ICP-MS- Inductively Coupled Plasma Mass Spectrometry

BET- (Brunauer, Emmett, and Teller) specific surface

OER- Oxygen Evolution Reaction

CV- Cyclic Voltammetry

LSV- Linear Sweep Voltammetry

EIS- Electrochemical Impedance Spectroscopy

CA- Chronoamperometry

CDL- Double Layer Capacitance

ECSA- Electrochemically active surface area

RHE- Reversible Hydrogen Electrode

RP- Ruddlesden-Popper phase